Cell, Vol. 104, 781–790, March 9, 2001, Copyright ©2001 by Cell Press

Structural Basis of Caspase Inhibition by XIAP: Differential Roles of the Linker versus the BIR Domain

Yihua Huang,†‖ Young Chul Park,*‖
Rebecca L. Rich,‡ Deena Segal,*
David G. Myszka,‡ and Hao Wu*§
*Department of Biochemistry
Weill Medical College of Cornell University and
†Program in Physiology, Biophysics
and Molecular Medicine
Graduate School of Medical Sciences
of Cornell University
1300 York Avenue
New York, New York 10021
‡Center for Biomolecular Interaction Analysis
School of Medicine
University of Utah
Salt Lake City, Utah 84132

Summary

The inhibitor of apoptosis proteins (IAPs) represent the only endogenous caspase inhibitors and are characterized by the presence of baculoviral IAP repeats (BIRs). Here, we report the crystal structure of the complex between human caspase-7 and XIAP (BIR2 and the proceeding linker). The structure surprisingly reveals that the linker is the only contacting element for the caspase, while the BIR2 domain is invisible in the crystal. The linker interacts with and blocks the substrate groove of the caspase in a backward fashion, distinct from substrate recognition. Structural analyses suggest that the linker is the energetic and specificity determinant of the interaction. Further biochemical characterizations clearly establish that the linker harbors the major energetic determinant, while the BIR2 domain serves as a regulatory element for caspase binding and Smac neutralization.

Introduction

Induction of programmed cell death or apoptosis is crucial for many aspects of biological functions in multicellular organisms, including maintenance of cellular homeostasis, fetal development, and immune system regulation (Steller, 1995; Thompson, 1995). Failure to control apoptosis can lead to serious diseases that threaten the existence of the organism. For example, the downregulation of apoptosis is often associated with cancer and autoimmune diseases. The upregulation of apoptosis is observed in many forms of degenerative disorders such as Alzheimer's disease, ischemic injury from stroke, and post menopausal osteoporosis. During viral infection, apoptosis is also a central combating element, as host cells attempt to commit suicidal apoptotic cell death and viruses counteract by expressing anti-apoptotic proteins.

§To whom correspondence should be addressed (haowu@med.cornell.edu).
‖These authors contributed equally to the work.

The eliciting of caspase activities represents an evolutionarily conserved point of apoptotic cell death. These novel cysteine proteases specific for aspartic residues are the major players that disable homeostatic and repair processes, halt cell cycle progression, mediate structural disassembly and morphological changes, and mark the dying cell for engulfment and disposal (Nicholson, 1999). Caspases are synthesized as proenzymes that are activated by specific cleavages after Asp residues, either via auto-processing or a caspase cascade, to generate mature caspases with an $\alpha 2\beta 2$ stoichiometry. Based on substrate specificity, caspases can be divided into three groups, the inflammation group, the apoptotic effector group, and the apoptotic initiator group (Nicholson, 1999).

The importance of caspases in apoptosis necessitates that these potentially dangerous enzymes are highly regulated by both cellular and viral inhibitors. The inhibitors of apoptosis proteins (IAPs), which have been identified in diverse organisms, are the only known endogenous caspase inhibitors that effectively suppress programmed cell death. There are currently seven human IAPs, including X chromosome linked IAP (XIAP), c-IAP1, c-IAP2, NAIP, Survivin, BRUCE, and ML-IAP (Rothe et al., 1995; Duckett et al., 1996; Liston et al., 1996; Ambrosini et al., 1997; Deveraux et al., 1997; Hauser et al., 1998; Vucic et al., 2000). IAPs are characterized by the presence of one to three tandem baculoviral IAP repeats (BIRs) (Crook et al., 1993; Deveraux and Reed, 1999; Miller, 1999), which exhibit a structural architecture of classical zinc fingers as shown by structural studies (Hinds et al., 1999; Sun et al., 1999; Chantalat et al., 2000; Liu et al., 2000; Muchmore et al., 2000; Verdecia et al., 2000; Wu et al., 2000).

Overexpression of almost all IAPs has been shown to suppress apoptosis induced by a variety of stimuli such as death receptor activation, growth factor withdrawal, and cytotoxic insults (Deveraux and Reed, 1999). In vivo, IAP expression is deregulated in many forms of human cancers, further strengthening the role of IAPs as cell death inhibitors and their relevance in human diseases (Deveraux and Reed, 1999; Hay, 2000). In addition, it has been shown by genetic knockout in mice that endogenous NAIP is required for neuronal survival in pathological conditions (Holcik et al., 2000). In *Drosophila*, IAP function is essential for cell survival (Miller, 1999; Hay, 2000). However, only three mammalian IAPs, XIAP, c-IAP1, and c-IAP2 have been shown to exhibit direct inhibitory activity toward caspases (Deveraux et al., 1997; Roy et al., 1997), while other IAPs such as survivin may play important roles in microtubule organization during mitosis (Uren et al., 2000).

IAPs may exploit several different mechanisms for caspase inhibition. For example, XIAP, c-IAP1, and c-IAP2 are direct inhibitors of activated effector caspases such as caspase-3 and caspase-7 (Deveraux et al., 1997; Roy et al., 1997). They are also potent inhibitors for the proteolytic activation of caspase-9, an initiator caspase (Deveraux et al., 1998, 1999). Some IAPs also contain a RING domain, which appears to act as a ubi-

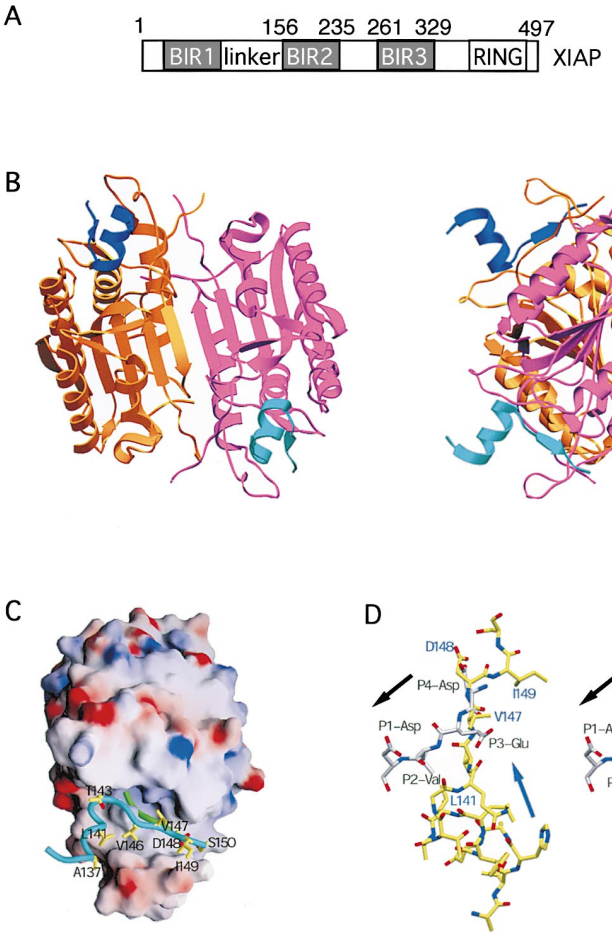

Figure 1. Overview of the XIAP/Caspase-7 Complex

(A) Schematic domain organization of XIAP.

(B) Ribbon drawings of the XIAP/caspase-7 complex, shown looking down the 2-fold axis (left) and with the 2-fold axis horizontal (right). The caspase-7 protomers are shown in magenta and orange and the XIAP molecules are in cyan and blue.

(C) Electrostatic surface representation of caspase-7 and the bound worm model of XIAP linker (cyan) and a tetra-peptide substrate inhibitor (green). Selected side chains in XIAP are shown as stick models.

(D) Stereo view of superimposed XIAP linker and a substrate inhibitor bearing the DEVD sequence, showing the backward binding of the linker and the spatial overlap for competitive inhibition. The chain directions for the linker (blue arrow) and the substrate (black arrow) are shown.

quitin ligase for the degradation of bound caspases (Yang et al., 2000). Therefore, IAPs put brakes on the apoptotic process by inhibiting caspase activity and maturation and perhaps by degrading caspases (Green, 2000).

It has been shown recently that the caspase inhibitory function of IAPs may be relieved by a newly identified novel mitochondrial protein Smac/DIABLO (Du et al., 2000; Verhagen et al., 2000). Smac is released into the cytosol during apoptosis and decreases the cellular threshold for apoptotic stimuli. It appears to be a functional homolog of the *Drosophila* proteins Reaper, Hid, and Grim, which are also IAP neutralizers (Hay, 2000). The biochemical basis of Smac function relies on a direct physical association with multiple IAPs (Chai et al., 2000; Du et al., 2000; Liu et al., 2000; Verhagen et al., 2000; Wu et al., 2000).

Previous biochemical dissection of XIAP showed that a region containing its second BIR (linker-BIR2, residues 124–240) is a minimal functional unit for the inhibition of effector caspases such as caspase-3 and -7 (Takahashi et al., 1999). However, it is not clear how this inhibition is achieved. To understand the molecular basis of XIAP function, we obtained the crystal structure of the complex between this region of human XIAP and human caspase-7. The structure surprisingly revealed that the linker is the only contacting element for the caspase, while the BIR2 domain is completely invisible in the crystal. A model of caspase-7 in complex with both the linker and the BIR2 domain suggests that such BIR2/caspase-7 interface would have been in steric clash with crystal packing. The linker interacts with the substrate groove of the caspase in a backward fashion that is completely different from substrate recognition and indirectly blocks the active site. Structural analyses of the linker/caspase-7 interaction provide an explanation for the mutual specificity between XIAP, c-IAP1, and c-IAP2 and the effector caspases. Further biochemical and biophysical characterizations using GST pull-down and surface plasmon resonance clearly showed that the linker harbors the major energetic determinant for caspase binding, while the BIR2 domain per se is both necessary and sufficient for Smac interaction. Therefore, the BIR2 domain acts as a regulatory element, which, on one hand, strengthens the linker interaction for the caspase and, on the other hand, senses the release of Smac by direct physical interaction. The weaker affinity of BIR2 for caspases facilitates Smac binding to BIR2, which makes BIR2 a convenient peeling point for destabilizing the XIAP/caspase interaction. This function of the BIR2 domain in XIAP may be general for other BIR domains in IAP proteins and further suggests that the BIR domains may not represent signatures for caspase inhibition, but rather serve as structural architectures for the evolution of diverse biological functions.

Table 1. Crystallographic Statistics

X-Ray Data	
X-ray source	CHESS F1
Wavelength (Å)	0.948
Temperature (K)	100
Space group	$P3_221$
Cell dimensions (Å)	a = b = 88.5, c = 185.4
Resolution (Å)	2.4
R_{sym} (last shell) (%)	5.2 (33.9)
Completeness (last shell) (%)	99.3 (99.5)
Molecular Replacement	
Resolution (Å)	10–3.8
Correlation coefficient	48.0
R_{MR} (%)	40.8
$R_{rigid\text{-}body}$ (R_{free}) (%)	36.6 (38.1)
Refinement	
Resolution (Å)	20–2.4
Sigma cutoff	1.5
Number of protein residues	501
Number of protein atoms	3,925
Number of solvent atoms	201
Number of reflections used	28,151
R (R_{free}) (%)	22.4 (26.0)
RMSD bond length (Å)	0.009
RMSD bond angle (°)	1.571
RMSD bond B factor (Å^2)	2.002
RMSD angle B factor (Å^2)	3.068

Results

Overview of the XIAP/Caspase-7 Complex: Backward Binding of the Linker and Invisibility of the BIR2 Domain

Crystal structure of the complex between human caspase-7 and a functional unit of XIAP containing the BIR2 domain and the proceeding linker region (linker-BIR2, residues 120–260) was determined at 2.4 Å resolution (Figures 1A and 1B and Table 1). The structure surprisingly revealed that the linker contains the only contacting element for the caspase, while the BIR2 domain is completely invisible in the crystal from either of the two independent XIAP/caspase-7 interactions. However, an SDS-PAGE analysis of re-dissolved crystals confirmed the integrity of the linker-BIR2 protein in these crystals (data not shown).

In the complex, the linker peptide exhibits an $\alpha + \beta$ conformation and binds to the substrate groove on the surface of caspase-7, in a manner unlike "canonical" substrate interaction in a Michaelis-Menton complex. This is in contrast to a previous suggestion that a sequence within the linker region (148-DISD-151) binds as a pseudo-substrate into the active site of their target caspases (Sun et al., 1999). In fact, the main chain of the linker peptide deviates from and runs almost antiparallel with the course taken by substrate-based peptide inhibitors (Figures 1C and 1D). The side chains of the linker peptide that are crucial for caspase interaction do not interact with the well-characterized S4–S1 pockets, but simply spatially overlap with the substrate residues. Therefore, XIAP does not directly block the active center as a pseudo-substrate, but indirectly causes competitive inhibition by overlapping with substrate binding.

The invisibility of the BIR2 domain in the crystal suggests that the linker is the major energetic determinant of the XIAP/caspase interaction, in contrast to the previous belief that the conserved BIR domains play dominant roles in caspase inhibition (Deveraux and Reed, 1999). However, the BIR2 domain does appear to interact with caspase-7 in solution, as limited proteolysis of the complex with trypsin, chymotrypsin, and subtilisin failed to cleave off the BIR2 domain. These observations suggest that the BIR2 domain per se may possess low affinity to the caspase (see below) and the binding may be replaced by favorable packing interactions in the crystal. The C-terminal end of the linker, which the BIR2 domain is attached to, resides at the edge of a large solvent channel in the crystal. This would therefore permit the flex of the unbound BIR2 domain within this solvent space and hence lead to the observed crystallographic disordering. Similar competition between low-affinity binding interactions and crystal packing interactions has been observed in several low-affinity TRAF2-peptide crystal structures (Park et al., 1999; Ye et al., 1999).

Structural Determinant of the XIAP/Caspase-7 Interaction

Residues 134–150 of XIAP are visible in the complex, out of which residues 137–150 make direct contact with the caspase. The peptide begins as an α-helical conformation and switches into an extended conformation after residue 145. The interaction buries 700 Å^2 surface area from each of the binding partners and engages a total of 154 interfacial van der Waals contacts. Most of the atomic interactions are hydrophobic or mixed and involve hydrophobic residues (Figure 2A). The footprint of the linker interaction on caspase-7 overlaps with that of a caspase substrate (Figure 2B). There are only five intermolecular hydrogen bonds at each interface (Figure 2C). The two independent protomers of caspase-7 and the linker peptides are highly similar, which superimpose to rms distances of 0.35 Å and 0.20 Å, respectively.

Residue D148 of XIAP appears to be a major anchoring point for the interaction. Among the five well-defined intermolecular hydrogen bonds in the complex, three are made by D148 (Figure 2C and Table 2), while the remaining two are made by main chain atoms of the linker peptide. The side chain carboxylate of D148 makes hydrogen bonds to the Nϵ1 atom of residue W240 and the main chain amide nitrogen of Q276 of caspase-7, respectively. The main chain amide nitrogen of this residue is also within hydrogen bonding distance to the carbonyl oxygen of R233 of caspase-7. Even though D148 situates near the S4 site, its interaction with the caspase is quite different from the recognition of a P4 Asp by the caspase. In a complex between caspase-7 and a substrate-based inhibitor bearing the P4-DEVD-P1 sequence, the P4 Asp makes three hydrogen bonds exclusively to Q276 (Wei et al., 2000). One side chain carboxyl atom of the P4 Asp makes two hydrogen bonds with the main chain and side chain amide atoms of Q276, while the main chain amide nitrogen of the residue interacts with the main chain carbonyl atom of Q276.

Unlike the highly ionic nature of substrate/caspase interactions, the remaining interactions by the linker peptide are mostly hydrophobic (Figure 2A and Table 2). Side chains on one side of the helix including residues A137, L141, and V146 interact tightly with a hydrophobic patch formed by T189, Y230, W232, and F282 of cas-

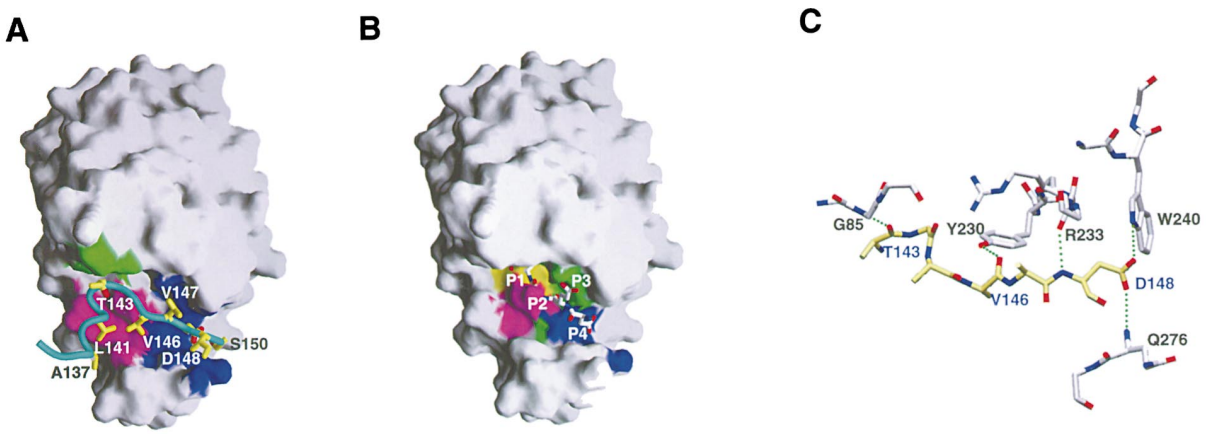

Figure 2. Details of the XIAP/Caspase-7 Interaction

(A) The molecular footprint of XIAP on caspase-7. Magenta: footprint for residues A137, L141, and V146. Green: footprint for residues R142, T143, and G144. Blue: footprint for residues V147–S150.

(B) The molecular footprint of a tetra-peptide inhibitor (Ac-DEVD-CHO) for comparison. Colors yellow, magenta, green, and blue are for P1–P4 residues, respectively.

(C) Hydrogen bonding interactions between the linker (yellow) and caspase-7 (gray). Side chains for T143 and V146 of XIAP are omitted for clarity.

pase-7 at the base of the surface groove. The other side of the helix, including the main chain of R142, residue T143, and G144, contacts the top wall of the groove at residues G83, M84, and H144 of caspase-7. The remaining of the peptide, including residues V147, D148, I149, and S150, contacts the other end of the surface groove formed by caspase-7 residues R233, W240, Q276, and S277.

Based on the surface area burial and specific hydrogen bonds, residues L141, V146, V147, D148, and I149 form the key structural determinant for the interaction. Among these residues, L141, V146, and D148 are almost completely buried in the complex with less than 10% surface area exposure (Figure 3A and Table 2). This analysis of the structural determinant of binding is consistent with previous alanine mutagenesis results on L141, V147, D148, and I149 (Sun et al., 1999). We predict that V146A mutation should also exhibit a strong effect on caspase binding. The specific hydrogen bonds formed by the side chain of D148 suggest that this residue has to be strictly conserved. For example, a D148N mutation may disrupt one of the hydrogen bonds as the side chain amide atom is not a good hydrogen bond acceptor and a D148E mutation may not be accommodated due to its larger size as the D148 residue is completely buried in the complex.

Regions in caspase-7 that contact the linker XIAP peptide are largely from the L1 loop, the L3 loop, the C-terminal tail of the large subunit, the L4 loop, the beginning of helix α4, and the L5 loop (Figure 3B and Table 2). Some of these regions, such as the L1 and the L5 loop, are highly variable structurally. Based on surface area burial and specific hydrogen bonds, we suggest that residues T189, Y230, R233, W240, Q276, and F282 are key determinants for XIAP binding. Among these residues, Y230 and F282 contribute most significantly to the large patch of hydrophobic surface at the bottom of the surface groove. The side chain of Y230 also contributes a specific hydrogen bond to the XIAP peptide. R233, W240, and Q276 form the hydrogen bonding network that anchors the D148 residue of XIAP.

Table 2. Surface Areas and Hydrogen Bonds in the XIAP/Capase-7 Complex

XIAP	Surface Area Burial (Å^2)	Fraction Exposure in Complex	Hydrogen Bonds
A137	42	0.21	O:N^{G85}
D138	0	0.47	
Y139	10	0.50	
L140	5	0.18	
L141	95	0.09	
R142	40	0.47	
T143	56	0.06	
G144	55	0.05	
Q145	22	0.33	
V146	75	0.07	O:Oη^{Y230}
V147	80	0.23	
D148	105	0.04	N:O^{R233}; Oδ1:N^{Q276}; Oδ2:Nϵ1^{W240}
I149	90	0.42	
S150	45	0.55	

The Linker/Caspase-7 Interaction Explains the Mutual Specificity of a Subset of IAP Family Members for Effector Caspases

The three groups of mammalian caspases defined based on substrate specificity are represented by caspase-1 for group I inflammation caspases, caspase-3 and caspase-7 for group II apoptotic effector caspases, and caspase-8 for group III apoptotic initiator caspases (Nicholson, 1999). Three members of the IAP family, XIAP, c-IAP1, and c-IAP2 have been shown to exhibit a distinct specificity for effector caspases (Deveraux et al., 1997, 1998; Roy et al., 1997; Takahashi et al., 1998). The structural basis of this mutual specificity can be explained by the sequence conservation of key residues at the interface between the linker of XIAP and human caspase-7.

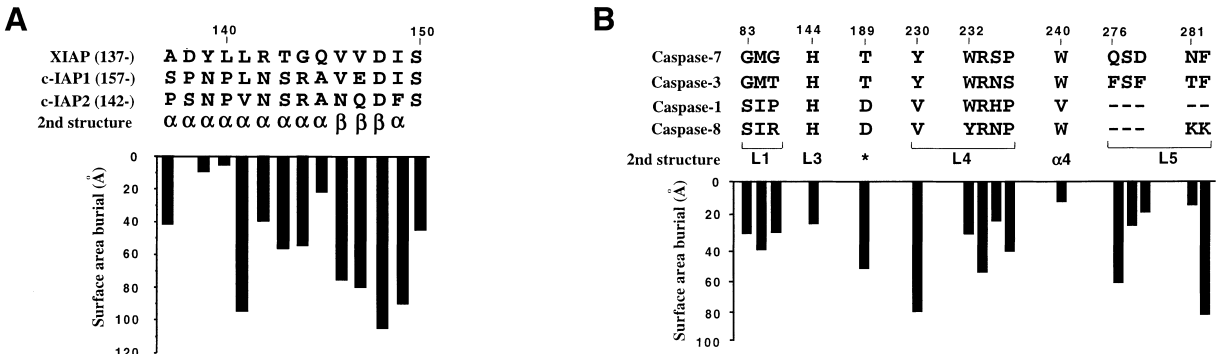

Figure 3. Sequence Conservation and Mutual Specificity of XIAP, c-IAP1, and c-IAP2 for Effector Caspases such as Caspase-3 and Caspase-7

(A) Sequence conservation among linker residues in XIAP, c-IAP1, and c-IAP2.

(B) Sequence conservation and variation among different caspases for residues interacting with XIAP. Secondary structure locations and surface area burials for these residues are also shown. *, C-terminal tail of the large subunit.

Among the different caspases, structure-based sequence comparison is possible for the four representative caspases (caspase-1, 3, 7, and 8), for which crystal structures are available (Walker et al., 1994; Mittl et al., 1997; Blanchard et al., 1999, 2000; Watt et al., 1999; Wei et al., 2000). Inclusive of all the contact residues for XIAP in caspase-7, the corresponding residues in caspase-3 are highly conserved (Figure 3B). In contrast, corresponding residues in caspase-1 and caspase-8 are less conserved. In particular, residue Q276, whose main chain amide nitrogen makes a direct hydrogen bond to the carboxylate of the XIAP anchoring residue D148, is absent in these caspases, as the L5 loop is much shorter than that in caspase-3 and caspase-7. Therefore, the linker of XIAP can only interact with the effector caspases. As the linker is the major structural determinant of caspase recognition (see below), this explains the structural basis of XIAP specificity.

The linker residues in XIAP can be superimposed with the corresponding linkers of c-IAP1 and c-IAP2 proceeding their BIR2 domains (Figure 3A), as also suggested earlier (Sun et al., 1999). In particular, the anchoring D148 residue of XIAP is absolutely conserved in this superposition. Residues L141, T143, and V146, which are completely buried at the interface and important for caspase interaction, are either identical or contain conservative substitutions. Side chains for residues R142, V147, and I149 are not completely buried and therefore may accommodate the sequence changes while maintaining most of the interaction. Searching of other IAPs for the presence of similar sequences did not yield any positive hits, further suggesting that not all members of the IAPs exhibit caspase inhibitory activity.

Structure-Based Biochemical Experiments Establish that the Linker Is the Major Energetic Determinant of the XIAP/Caspase Interaction, While the BIR2 Domain Plays a Facilitating Role

Previous biochemical studies suggest that at least one BIR domain from IAPs is required for caspase inhibition, suggesting a dominant role of the BIR domains in this function (Deveraux and Reed, 1999). The structural observation motivated us to systematically examine the role of the linker versus the BIR2 domain in the interaction with caspase-7. We generated a series of GST constructs that contain the linker-BIR2, the linker alone, and the BIR2 domain alone, and used these GST fusion proteins for the pulldown of caspase-7 (Figure 4A). These experiments clearly showed that the linker-BIR2 and the linker alone of XIAP significantly retained caspase-7 after extensive washing, while the BIR2 domain alone retained only a residual amount of caspase-7, suggesting that the BIR2 domain alone possesses much lower affinity to caspase-7 than the linker. In addition, compared to the linker alone, the linker-BIR2 appears to have retained caspase-7 more stoichiometrically, suggesting modest but significant energetic contribution from the BIR2 domain in the linker-BIR2 protein.

To quantitatively determine the differential affinities of these regions of XIAP with caspase-7, we captured the same GST fusion proteins onto the sensor chips by anti-GST antibodies for measurement by surface plasmon resonance (SPR). As the molar quantities of the GST fusion proteins on the chips are equal due to the specific capturing procedure, their interaction strengths to caspase-7 can be directly obtained and compared. These measurements showed that the linker-BIR2 protein exhibits a dissociation constant of 0.5 nM with caspase-7, and that the linker alone is 70-fold weaker, with a dissociation constant of 35 nM (Table 3). Interestingly, however, an earlier caspase inhibition assay showed that the linker peptide was not sufficient to exert caspase inhibition at a 1 μM concentration (Sun et al., 2000), in contrast to our observation. We suspect that the linker peptide may have existed as an aggregate in the absence of GST fusion due to its significant hydrophobic content or in a nonproductive conformation due to an intramolecular interaction involving the free termini, and is thus unable to interact with the caspase. Therefore, both qualitative and quantitative experiments presented here clearly established the dominant role of the linker and the facilitating role of the BIR2 domain in caspase interaction and inhibition.

Unlike the XIAP/Caspase Interaction, SPR Measurements Reveal that the BIR2 Domain Alone Determines Smac Binding

Smac is a mitochondrial protein that gets released into the cytosol during the initiation of apoptosis and antago-

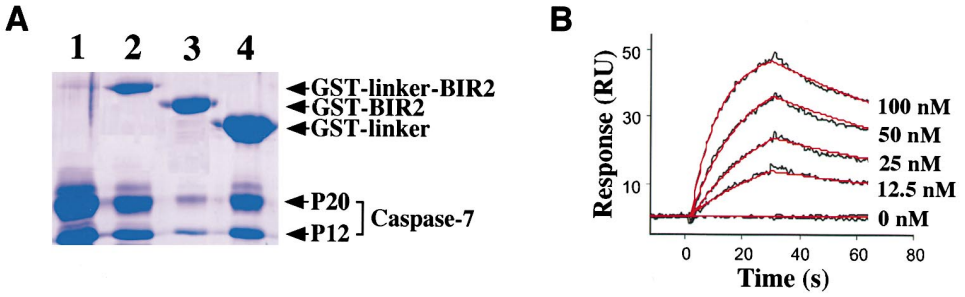

Figure 4. Biochemical and Biophysical Characterization of the XIAP/Caspase-7 and XIAP/Smac Interactions

(A) GST pulldown analysis of the XIAP/caspase-7 interaction. Lane 1: input caspase-7, Lanes 2–4: pulldown of caspase-7 by GST-linker-BIR2, GST-BIR2, and GST-linker of XIAP, respectively.

(B) A representative overlay of the surface plasmon resonance sensogram of the XIAP/Smac interaction.

nizes IAP function by physical interactions with IAPs to relieve caspase inhibition (Chai et al., 2000; Du et al., 2000; Liu et al., 2000; Verhagen et al., 2000; Wu et al., 2000). Previous biochemical studies showed that Smac interacts strongly with many BIR domain constructs from different IAPs. However, as these experiments used generous domain constructs that usually contain significant peripheral residues beyond a BIR domain defined either by sequence or structure, it is necessary to re-examine some of these experiments in light of the potential role of peripheral or linker residues in these protein–protein interactions.

The same comparative binding experiments using SPR between GST fusion XIAP fragments and caspase-7 were also performed for the interaction between XIAP and Smac (Figure 4B and Table 3). The experiments showed that the BIR2 domain alone is both necessary and sufficient for Smac binding (K_D = 35 nM), while the linker does not contribute to this binding. This is shown both by the similar affinity of Smac to either BIR2 alone or to linker-BIR2 of XIAP and by the lack of binding of the linker to Smac. This is in contrast to the weak affinity between BIR2 alone and caspase-7, making Smac a much stronger competitor for BIR2 binding than caspase-7.

The BIR2 Domain of XIAP Appears to Function as a Regulatory Domain in Caspase Binding and in Relieving Caspase Inhibition by Smac

BIR domains are conserved motifs of around 70 residues in length that exhibit a structural architecture of classical zinc fingers. Our structural and biochemical characterizations of the XIAP/caspase interaction established that the linker region harbors the major energetic and specificity determinant for caspase interaction/inhibition, and raised the hypothesis that the BIR2 domain of XIAP functions as a regulatory element for caspase inhibition.

The interaction of XIAP with a target caspase is bipartite, involving both the linker region and the BIR2 domain. This mode of protease inhibition by binding near both the active site and an exosite bears similarity to the inhibition of several papain-like cysteine proteases (Bode and Huber, 2000). During caspase binding, as the linker possesses higher affinity to the caspase, it is most likely to be the binding initiator for the interaction. Upon linker binding, the BIR2 domain, which possesses much weaker affinity to the caspase, would subsequently latch onto the caspase to stabilize the interaction. Based on the BIR2 domain residues that have undergone chemical shift perturbations upon the introduction of caspase-3, we obtained a model of the linker-BIR2/caspase-7 interaction (Figure 5A). This was done first through manual docking and then refined using molecular dynamics simulations that incorporate the available chemical shift data and limited mutagenesis data (Sun et al., 1999). This BIR2/caspase-7 interaction is largely independent of the maturation state of the caspase, as shown by the similar pattern of chemical shift perturbations by procaspase-3 (Sun et al., 1999). The model confirmed that such a complex would have been in steric clash with a neighboring molecule in the crystal lattice for both independent XIAP/caspase interactions, which would shove the BIR2 domain into the neighboring solvent space in the crystal lattice.

The sequence similarity between the BIR2 and BIR3 domains of XIAP allowed us to map the interacting residues for Smac onto the surface of the BIR2 domain based on a structure of the BIR3/Smac complex (Liu et al., 2000; Wu et al., 2000) (Figure 5B). This interface, interestingly, overlaps with residues implicated for caspase-3 binding from chemical shift measurements. Therefore, Smac may directly compete with caspases for XIAP binding. As the BIR2 domain per se possesses much higher affinity for Smac than for a target caspase, Smac apparently is a highly efficient competitor for BIR2 binding. Once BIR2 is stripped off the caspase by Smac binding, the linker would either be insufficient to maintain caspase binding and inhibition, or be removed off the caspase through steric hindrance from the Smac protein.

These observations suggest a model of caspase inhibition by XIAP and perhaps other related IAPs that highlights the regulatory role of the BIR2 domain in this

Table 3. SPR Measurements of XIAP/Caspase-7 and XIAP/Smac Interactions

Protein on Chip	Protein in Solution	Dissociation Constant (K_D)
GST-linker-BIR2 (124–240)	Caspase-7	0.5 nM
GST-linker (124–159)		35 nM
GST-linker-BIR2 (124–240)	Smac	15 nM
GST-BIR2 (156–240)		35 nM
GST-linker (124–159)		No binding

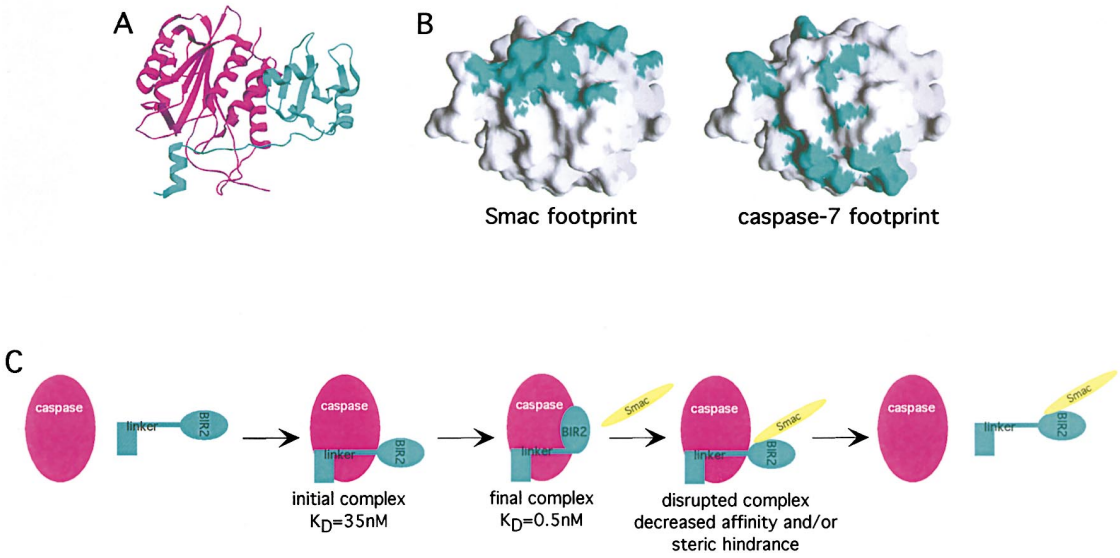

Figure 5. Molecular Mechanism of Caspase Inhibition by XIAP and Other Related IAPs

(A) A model of the linker-BIR2/caspase-7 complex, obtained by manual docking and restrained molecular dynamics simulations. Only half of a dimeric complex is shown. Magenta: caspase-7; cyan: linker-BIR2. The BIR2 domain within the complex would be in steric clash with a neighboring molecule in the current crystal.

(B) Mapping of BIR2 residues in contact with Smac (left), based on a homologous BIR3/Smac complex (Wu et al., 2000), and in contact with a target caspase (right), based on NMR chemical shift data (Sun et al., 1999), showing the overlap and therefore the competition of the two interactions.

(C) A schematic model for the molecular mechanism of the interplay between a caspase, XIAP, or other related IAPs and Smac, showing the regulatory role of the BIR2 domain.

process (Figure 5C). During caspase interaction and inhibition, the BIR2 domain helps to stabilize the initial interaction of the linker near the active site of the caspase by binding to an adjacent site. When Smac is released into the cytosol from the mitochondria during the initiation of apoptosis, it binds the BIR2 domain of XIAP, among other BIR domains. As Smac possesses high affinity to the BIR2 domain, this interaction would easily compete off the binding of BIR2 to a target caspase and subsequently causes the liberation of the caspase from the grip of XIAP. Our crystal structure of the linker/caspase-7 interaction is likely to have captured a glimpse of one step in this process in which the BIR2 domain has been peeled off from the caspase, by Smac in vivo and by crystal packing in the crystal. Therefore, even though the BIR2 domain is not the energetic determinant of caspase binding, it is the major responder to Smac regulation. In this regard, as Smac appears to interact with many BIR domains, this function of BIR domains may be a major role for the conservation of these domains among the IAP family members. Once Smac relieves the inhibitory activity of some IAPs, the uninhibited caspases would further amplify the pro-apoptotic process by cleaving and perhaps degrading additional IAPs (Deveraux et al., 1999).

Discussion

General Roles for BIR Domains and Linker Residues in Caspase Inhibition?

Our crystal structure of the complex between XIAP (linker-BIR2) and caspase-7 surprisingly revealed that the linker is the major determinant of binding and inhibition for the caspase. The linker interacts specifically with the substrate binding groove of the caspase in a backward manner from what is seen in a regular substrate. The interaction spatially overlaps with substrate recognition and creates competitive inhibition with caspase substrates. Backward binding has been observed for synthetic small peptide inhibitors of the cysteine protease papain (LaLonde et al., 1998). However, this mode of inhibitor binding is generally rather rare and we are not aware of any cases of such binding interactions for endogenous protease inhibitors. The revelation of the interaction of an XIAP peptide with the caspase also raises the possibility of therapeutic intervention for relieving IAP functions in the treatment of cancer and other proliferative diseases.

On the other hand, the BIR2 domain of XIAP is completely invisible in the crystal. Our structural and biophysical analyses suggest that this domain per se possesses low affinity to the target caspase. Thus, the interaction between BIR2 and the caspase in solution may have been competed off by packing interactions in the crystal. This weak affinity creates a convenient peeling point for relieving the inhibition of XIAP by the Smac protein, as Smac/BIR2 interaction possesses higher affinity than the caspase/BIR2 interaction. A direct competition of Smac to the high-affinity caspase binding by the linker-BIR2 or full-length XIAP would have been much more difficult. Therefore, the BIR2 domain functions as a regulatory element for caspase inhibition by being the stabilizer for caspase binding and the responder for Smac binding.

The current structural observation raises the question whether the differential roles of the linker versus the BIR

domain represent a general phenomenon for other IAP/caspase interactions. As shown by the sequence homology of the XIAP linker with the linker regions of c-IAP1 and c-IAP2, this might be true for the inhibition of caspase-3 and caspase-7 by these IAPs as well. The situation for caspase-9 inhibition by the BIR3 domain of XIAP is less clear (Deveraux et al., 1999; Sun et al., 2000). Similar to other dissection experiments, the definition of the BIR3 domain used for caspase-9 inhibition is also more liberal than the BIR domain per se. In the NMR structure of the BIR3 domain of XIAP, an additional C-terminal α helix is observed in comparison with the BIR2 domain structure. Based on the mutagenesis results, this additional helix harbors at least one crucial residue for caspase-9 interaction (Sun et al., 2000), which may be a major determinant for this inhibition. Further structural studies of the complex would be required to determine the molecular basis of this interaction.

Linker or Peripheral Residues as Convenient Evolutionary Units?

BIR domains present in IAPs are classical zinc fingers that are involved in numerous protein–DNA and protein–protein interactions. In this regard, perhaps it is not surprising to note that these domains may simply serve as structural architectures for the evolution of new functions. For example, the role of peripheral residues outside the BIR domains has also been observed in a different context other than caspase inhibition, which relates to survivin, an IAP family member with a specific function in mitosis. The crystal structure of the protein, which is dimeric in solution, showed that the protomer structure has an additional long C-terminal helix beyond the BIR domain. This helix and the loop in between surprisingly form a majority of the dimerization interface (Chantalat et al., 2000; Muchmore et al., 2000; Verdecia et al., 2000).

Many conserved protein domains have been implicated in important biological functions. An example of the significance of peripheral residues around these domains has been provided by the crystal structure of the complex between the death domains of Pelle and Tube (Xiao et al., 1999). Death domains are protein–protein interaction modules involved in death receptor signaling in mammals. In *Drosophila*, the serine/threonine kinase Pelle interacts with the adaptor protein Tube through their death domains, which leads to the activation of the transcription factor Dorsal during embryogenesis. The crystal structure of the complex surprisingly showed that an interhelical insertion and the C-terminal tail of the Tube death domain make indispensable contacts in the heterodimer. Collectively, these observations suggest that conserved domains may serve as structural scaffolds for the evolution of new functions from their peripheral residues. These linear peripheral sequences are perhaps much easier to evolve than modifications to a three-dimensional structure.

Experimental Procedures

Protein Expression and Purification

Human caspase-7 (cDNA obtained from an EST clone through the Genome Systems) was produced with a carboxy-terminal polyhistidine tag in *E. coli* by coexpressing the two fragments (residues M1-D206 and residues A207-Q303) that correspond to the first maturation cleavage. The expressed protein was autoprocessed to remove the short N-terminal pro-domain. The purification involves Ni-affinity chromatography, ion-exchange, and gel filtration. Human XIAP linker-BIR2 (residues 120–260) was expressed as a GST fusion protein and purified by glutathione beads. The GST tag was cleaved by thrombin and the reaction mixture was mixed with caspase-7 for complex formation. The thus obtained XIAP/caspase-7 complex was purified from GST by glutathione beads and from excess XIAP by gel filtration. Human Smac containing a carboxy-terminal polyhistidine tag was expressed and purified as described earlier (Wu et al., 2000). For biosensor experiments, GST fusion proteins of various XIAP constructs, including GST-linker-BIR2 (residues 124–240), GST-BIR2 (residues 156–240), and GST-linker (residues 124–159), were expressed and purified similarly to as described for the GST-linker-BIR2 protein (residues 120–260) used for crystallization.

Crystallization and Structure Determination

The complex containing XIAP (residues 120–260) and caspase-7 was concentrated to approximately 7 mg/ml in 20 mM Tris-HCl at pH 8.0, 300 mM NaCl, and 5 mM DTT and crystallized with hanging drop vapor diffusion using 20%–30% butanol. Diffraction data were collected at the CHESS F1 station under cryo-protected conditions and processed with the HKL package (Otwinowski and Minor, 1997) (Table 1). The structure was determined by molecular replacement calculations with the program REPLACE (Tong, 1993). The atomic model used for the search was modified from a human caspase-3 structure (PDB code 1CP3) in which residues different from the caspase-7 sequence were replaced by alanines. The rotation function gave a rather clear solution at 5.5 σ in height, in comparison with the next peak at 3.5 σ. However, to ensure thoroughness of the search, a total of 66 top rotation function grid points were searched for translation solutions. Summary statistics for the search and the rigid body refinement are shown in Table 1.

To locate the BIR2 domain in the crystal, atomic models from both the NMR structure of the BIR2 domain (PDB code 1C9Q) and the crystal structure of the BIR3 domain (PDB code 1G73) of XIAP were used, without producing any sensible solutions. On the other hand, a difference Fourier map calculated with phases from the human caspase-3 model, which was refined using conjugate gradient protocol only ($R = 34.6\%$, $R_{free} = 37.0\%$), showed clear electron densities near the substrate binding groove for the linker of XIAP. The structure was modeled using O (Jones et al., 1991) and further refined by the CNS program (Brunger et al., 1998). The final atomic model contains residues 55–196 and 211–303 from the first caspase-7 protomer, residues 58–196 and 211–303 from the second caspase-7 protomer, and residues 134–150 for both bound XIAP linkers. Ribbon drawings and stick models were produced in the program Setor (Evans, 1993) and surface plots were made by Grasp (Nicholls et al., 1991).

Surface Plasmon Resonance Experiments

All surface plasmon resonance measurements were performed at 20°C using a BIACORE 2000 equipped with a research-grade B1 sensor chip. The immobilization buffer was 10 mM HEPES, 150 mM NaCl, 0.005% P20, pH 7.4; the running buffer was 20 mM Tris, 150 mM NaCl, 2 mM DTT, 0.1 mg/ml BSA, 0.05% P20, pH 7.5. The GST fusion proteins of XIAP were captured at densities of ~300 RU by anti-GST monoclonal antibody (Biacore AB, Uppsala, Sweden) immobilized on the sensor chip surface. The surfaces of four flow cells were activated for 1 min with a 1:1 mixture of 0.1 M NHS (N-hydroxy-succinimide) and 0.1 M EDC (N-ethyl-N′-3-N,N-dimethyl-aminopropyl carbodiimide) at a flow rate of 20 μl/min. The antibody at a concentration of 50 μM in 10 mM sodium acetate, pH 5.0 was immobilized at a density of ~5000 RU on the four flow cell surfaces. Residual binding sites within the flow cells were blocked with a 7 min injection of 1.0 M ethanolamine at pH 8.0. Each GST construct was captured on the surface by injecting 5 μl of the construct in running buffer over the antibody at 5 μl/min for 1 min. Complete regeneration of the antibody surface was accomplished by an 18 s injection of glycine at pH 2.2.

To collect kinetic binding data, concentration series of the Smac and caspase-7 in running buffer were injected over the ligand and

reference flow cells at a flow rate of 50 μl/min. During each injection, the ligand/analyte complex was allowed to associate and dissociate for 30 and 60 s. All response data were double referenced (Myszka, 1999), thereby correcting for bulk refractive index changes and nonspecific analyte binding to the sample and reference surfaces. Data were fit globally to a simple interaction model (A + B = AB) using CLAMP (Myszka and Morton, 1998).

Acknowledgments

We thank the MacCHESS staff and Craig Ogata for synchrotron beam time and support, Hong Ye and Guozhou Xu for technical help, Benoit Roux for molecular dynamics simulations, and Yigong Shi for the His-tagged Smac construct. The work was supported by the Speaker's Fund for Biomedical Research and the departmental startup fund. Y. C. P is a postdoctoral fellow of the Cancer Research Institute and H. W. is a Pew Scholar of Biomedical Sciences.

Received February 14, 2001; revised February 22, 2001.

References

Ambrosini, G., Adida, C., and Altieri, D.C. (1997). A novel anti-apoptosis gene, survivin, expressed in cancer and lymphoma. Nat. Med. *3*, 917–921.

Blanchard, H., Kodandapani, L., Mittl, P.R., Marco, S.D., Krebs, J.F., Wu, J.C., Tomaselli, K.J., and Grutter, M.G. (1999). The three-dimensional structure of caspase-8: an initiator enzyme in apoptosis. Structure Fold. Des. *7*, 1125–1133.

Blanchard, H., Donepudi, M., Tschopp, M., Kodandapani, L., Wu, J.C., and Grutter, M.G. (2000). Caspase-8 specificity probed at subsite S(4): crystal structure of the caspase-8-Z-DEVD-cho complex. J. Mol. Biol. *302*, 9–16.

Bode, W., and Huber, R. (2000). Structural basis of the endoproteinase-protein inhibitor interaction. Biochim. Biophys. Acta *1477*, 241–252.

Brunger, A.T., Adams, P.D., Clore, G.M., DeLano, W.L., Gros, P., Grosse-Kunstleve, R.W., Jiang, J.S., Kuszewski, J., Nilges, M., Pannu, N.S., et al. (1998). Crystallography & NMR system: a new software suite for macromolecular structure determination. Acta Crystallogr. *D54*, 905–921.

Chai, J., Du, C., Wu, J.W., Kyin, S., Wang, X., and Shi, Y. (2000). Structural and biochemical basis of apoptotic activation by Smac/DIABLO. Nature *406*, 855–862.

Chantalat, L., Skoufias, D.A., Kleman, J.P., Jung, B., Dideberg, O., and Margolis, R.L. (2000). Crystal structure of human survivin reveals a bow tie-shaped dimer with two unusual alpha-helical extensions. Mol. Cell *6*, 183–189.

Crook, N.E., Clem, R.J., and Miller, L.K. (1993). An apoptosis-inhibiting baculovirus gene with a zinc finger-like motif. J. Virol. *67*, 2168–2174.

Deveraux, Q.L., and Reed, J.C. (1999). IAP family proteins—suppressors of apoptosis. Genes Dev. *13*, 239–252.

Deveraux, Q.L., Takahashi, R., Salvesen, G.S., and Reed, J.C. (1997). X-linked IAP is a direct inhibitor of cell-death proteases. Nature *388*, 300–304.

Deveraux, Q.L., Roy, N., Stennicke, H.R., Van Arsdale, T., Zhou, Q., Srinivasula, S.M., Alnemri, E.S., Salvesen, G.S., and Reed, J.C. (1998). IAPs block apoptotic events induced by caspase-8 and cytochrome c by direct inhibition of distinct caspases. EMBO J. *17*, 2215–2223.

Deveraux, Q.L., Leo, E., Stennicke, H.R., Welsh, K., Salvesen, G.S., and Reed, J.C. (1999). Cleavage of human inhibitor of apoptosis protein XIAP results in fragments with distinct specificities for caspases. EMBO J. *18*, 5242–5251.

Du, C., Fang, M., Li, Y., Li, L., and Wang, X. (2000). Smac, a mitochondrial protein that promotes cytochrome c-dependent caspase activation by eliminating IAP inhibition. Cell *102*, 33–42.

Duckett, C.S., Nava, V.E., Gedrich, R.W., Clem, R.J., Van Dongen, J.L., Gilfillan, M.C., Shiels, H., Hardwick, J.M., and Thompson, C.B. (1996). A conserved family of cellular genes related to the baculovirus iap gene and encoding apoptosis inhibitors. EMBO J. *15*, 2685–2694.

Evans, S.V. (1993). SETOR: hardware-lighted three-dimensional solid model representations of macromolecules. J. Mol. Graph. *11*, 134–138.

Green, D.R. (2000). Apoptotic pathways: paper wraps stone blunts scissors. Cell *102*, 1–4.

Hauser, H.P., Bardroff, M., Pyrowolakis, G., and Jentsch, S. (1998). A giant ubiquitin-conjugating enzyme related to IAP apoptosis inhibitors. J. Cell Biol. *141*, 1415–1422.

Hay, B.A. (2000). Understanding IAP function and regulation: a view from Drosophila. Cell Death Differ. *7*, 1045–1056.

Hinds, M.G., Norton, R.S., Vaux, D.L., and Day, C.L. (1999). Solution structure of a baculoviral inhibitor of apoptosis (IAP) repeat. Nat. Struct. Biol. *6*, 648–651.

Holcik, M., Thompson, C.S., Yaraghi, Z., Lefebvre, C.A., MacKenzie, A.E., and Korneluk, R.G. (2000). The hippocampal neurons of neuronal apoptosis inhibitory protein 1 (NAIP1)-deleted mice display increased vulnerability to kainic acid- induced injury. Proc. Natl. Acad. Sci. USA *97*, 2286–2290.

Jones, T.A., Zou, J.-Y., Cowan, S.W., and Kjeldgaard, M. (1991). Improved methods for building models in electron density maps and the location of errors in those models. Acta Crystallgr. *A47*, 110–119.

LaLonde, J.M., Zhao, B., Smith, W.W., Janson, C.A., DesJarlais, R.L., Tomaszek, T.A., Carr, T.J., Thompson, S.K., Oh, H.J., Yamashita, D.S., Veber, D.F., and Abdel-Meguid, S.S. (1998). Use of papain as a model for the structure-based design of cathepsin K inhibitors: crystal structures of two papain-inhibitor complexes demonstrate binding to S′-subsites. J. Med. Chem. *41*, 4567–4576.

Liston, P., Roy, N., Tamai, K., Lefebvre, C., Baird, S., Cherton-Horvat, G., Farahani, R., McLean, M., Ikeda, J.E., MacKenzie, A., and Korneluk, R.G. (1996). Suppression of apoptosis in mammalian cells by NAIP and a related family of IAP genes. Nature *379*, 349–353.

Liu, Z., Sun, C., Olejniczak, E.T., Meadows, R.P., Betz, S.F., Oost, T., Herrmann, J., Wu, J.C., and Fesik, S.W. (2000). Structural basis for binding of Smac/DIABLO to the XIAP BIR3 domain. Nature *408*, 1004–1008.

Miller, L.K. (1999). An exegesis of IAPs: salvation and surprises from BIR motifs. Trends Cell Biol. *9*, 323–328.

Mittl, P.R., Di Marco, S., Krebs, J.F., Bai, X., Karanewsky, D.S., Priestle, J.P., Tomaselli, K.J., and Grutter, M.G. (1997). Structure of recombinant human CPP32 in complex with the tetrapeptide acetyl-Asp-Val-Ala-Asp fluoromethyl ketone. J. Biol. Chem. *272*, 6539–6547.

Muchmore, S.W., Chen, J., Jakob, C., Zakula, D., Matayoshi, E.D., Wu, W., Zhang, H., Li, F., Ng, S.C., and Altieri, D.C. (2000). Crystal structure and mutagenic analysis of the inhibitor-of-apoptosis protein survivin. Mol. Cell *6*, 173–182.

Myszka, D.G. (1999). Improving biosensor analysis. Mol. Recognit. *12*, 1–6.

Myszka, D.G., and Morton, T.A. (1998). CLAMP: a biosensor kinetic data analysis program. Trends Biochem. Sci. *23*, 149–150.

Nicholls, A., Sharp, K.A., and Honig, B. (1991). Protein folding and association: insights from the interfacial and thermodynamic properties of hydrocarbons. Proteins *11*, 281–296.

Nicholson, D.W. (1999). Caspase structure, proteolytic substrates, and function during apoptotic cell death. Cell Death Differ. *6*, 1028–1042.

Otwinowski, Z., and Minor, W. (1997). Processing of X-ray diffraction data collected in oscillation mode. Methods Enzymol. *276*, 307–326.

Park, Y.C., Burkitt, V., Villa, A.R., Tong, L., and Wu, H. (1999). Structural basis for self-association and receptor recognition of human TRAF2. Nature *398*, 533–538.

Rothe, M., Pan, M.G., Henzel, W.J., Ayres, T.M., and Goeddel, D.V. (1995). The TNFR2-TRAF signaling complex contains two novel proteins related to baculoviral inhibitor of apoptosis proteins. Cell *83*, 1243–1252.

Roy, N., Deveraux, Q.L., Takahashi, R., Salvesen, G.S., and Reed, J.C. (1997). The c-IAP-1 and c-IAP-2 proteins are direct inhibitors of specific caspases. EMBO J. *16*, 6914–6925.

Steller, H. (1995). Mechanisms and genes of cellular suicide. Science *267*, 1445–1449.

Sun, C., Cai, M., Gunasekera, A.H., Meadows, R.P., Wang, H., Chen, J., Zhang, H., Wu, W., Xu, N., Ng, S.C., and Fesik, S.W. (1999). NMR structure and mutagenesis of the inhibitor-of-apoptosis protein XIAP. Nature *401*, 818–822.

Sun, C., Cai, M., Meadows, R.P., Xu, N., Gunasekera, A.H., Herrmann, J., Wu, J.C., and Fesik, S.W. (2000). NMR structure and mutagenesis of the third bir domain of the inhibitor of apoptosis protein XIAP. J. Biol. Chem. *275*, 33777–33781.

Takahashi, R., Deveraux, Q., Tamm, I., Welsh, K., Assa-Munt, N., Salvesen, G.S., and Reed, J.C. (1998). A single BIR domain of XIAP sufficient for inhibiting caspases. J. Biol. Chem. *273*, 7787–7790.

Takahashi, N., Udagawa, N., and Suda, T. (1999). A new member of tumor necrosis factor ligand family, ODF/OPGL/TRANCE/RANKL, regulates osteoclast differentiation and function. Biochem. Biophys. Res. Commun. *256*, 449–455.

Thompson, C.B. (1995). Apoptosis in the pathogenesis and treatment of disease. Science *267*, 1456–1461.

Tong, L. (1993). REPLACE, a suite of computer programs for molecular-replacement calculations. J. Appl. Cryst. *26*, 748–751.

Uren, A.G., Wong, L., Pakusch, M., Fowler, K.J., Burrows, F.J., Vaux, D.L., and Choo, K.H. (2000). Survivin and the inner centromere protein INCENP show similar cell-cycle localization and gene knockout phenotype. Curr. Biol. *10*, 1319–1328.

Verdecia, M.A., Huang, H., Dutil, E., Kaiser, D.A., Hunter, T., and Noel, J.P. (2000). Structure of the human anti-apoptotic protein survivin reveals a dimeric arrangement. Nat. Struct. Biol. *7*, 602–608.

Verhagen, A.M., Ekert, P.G., Pakusch, M., Silke, J., Connolly, L.M., Reid, G.E., Moritz, R.L., Simpson, R.J., and Vaux, D.L. (2000). Identification of DIABLO, a mammalian protein that promotes apoptosis by binding to and antagonizing IAP proteins. Cell *102*, 43–53.

Vucic, D., Stennicke, H.R., Pisabarro, M.T., Salvesen, G.S., and Dixit, V.M. (2000). ML-IAP, a novel inhibitor of apoptosis that is preferentially expressed in human melanomas. Curr. Biol. *10*, 1359–1366.

Walker, N.P., Talanian, R.V., Brady, K.D., Dang, L.C., Bump, N.J., Ferenz, C.R., Franklin, S., Ghayur, T., Hackett, M.C., Hammill, L.D., et al. (1994). Crystal structure of the cysteine protease interleukin-1 beta-converting enzyme: a (p20/p10)2 homodimer. Cell *78*, 343–352.

Watt, W., Koeplinger, K.A., Mildner, A.M., Heinrikson, R.L., Tomasselli, A.G., and Watenpaugh, K.D. (1999). The atomic-resolution structure of human caspase-8, a key activator of apoptosis. Structure Fold. Des. *7*, 1135–1143.

Wei, Y., Fox, T., Chambers, S.P., Sintchak, J., Coll, J.T., Golec, J.M., Swenson, L., Wilson, K.P., and Charifson, P.S. (2000). The structures of caspases-1, -3, -7 and -8 reveal the basis for substrate and inhibitor selectivity. Chem. Biol. *7*, 423–432.

Wu, G., Chai, J., Suber, T.L., Wu, J.W., Du, C., Wang, X., and Shi, Y. (2000). Structural basis of IAP recognition by Smac/DIABLO. Nature *408*, 1008–12.

Xiao, T., Towb, P., Wasserman, S.A., and Sprang, S.R. (1999). Three-dimensional structure of a complex between the death domains of Pelle and Tube. Cell *99*, 545–555.

Yang, Y., Fang, S., Jensen, J.P., Weissman, A.M., and Ashwell, J.D. (2000). Ubiquitin protein ligase activity of IAPs and their degradation in proteasomes in response to apoptotic stimuli. Science *288*, 874–877.

Ye, H., Park, Y.C., Kreishman, M., Kieff, E., and Wu, H. (1999). The Structural basis for recognition of diverse receptor sequences by TRAF2. Mol. Cell *4*, 321–330.

Protein Data Bank ID Code

The atomic coordinates of the XIAP/caspase-7 structure have been deposited in the Protein Data Bank with the ID code 1I4O.